Journal of Catalysis **210,** 127–136 (2002)
doi:10.1006/jcat.2002.3670

Improved Metal-Support Interaction in $Pt/CeO_2–SiO_2$ Catalysts after Zinc Addition

J. Silvestre-Albero, F. Rodríguez-Reinoso, and A. Sepúlveda-Escribano[1]

Departamento de Química Inorgánica, Universidad de Alicante, Apartado 99, E-03080 Alicante, Spain

Received January 16, 2002; revised March 27, 2002; accepted May 2, 2002

The effect of reduction temperature on ceria-promoted platinum and platinum–zinc catalysts supported on silica has been studied on catalysts prepared from chlorine-free precursors and characterized by X-ray diffraction (XRD), temperature-programmed reduction (TPR), and X-ray photoelectron spectroscopy (XPS). Their catalytic behavior has been evaluated in the vapor-phase hydrogenation of toluene and of crotonaldehyde (2-butenal), after reduction at low (473 K) and high (773 K) temperatures. Catalytic results in the selective hydrogenation of crotonaldehyde show that the presence of Zn produces a fivefold increase in catalytic activity after high-temperature reduction over that with the monometallic catalyst. This promoting effect is accompanied with an increase in the selectivity for the C=O double bond hydrogenation to yield the corresponding unsaturated alcohol, crotyl alcohol (2-buten-1-ol).

Key Words: **Pt–Zn catalysts; CeO_2 promotion; SMSI effect; temperature-programmed reduction; selective hydrogenation.**

INTRODUCTION

The discovery of the strong metal–support interaction (SMSI) effect by Tauster *et al.* (1) gave rise to a huge amount of research work trying to find both an explanation and also new catalytic applications. The SMSI effect is characterized by the suppression of the H_2 and CO chemisorption ability of noble metals supported on reducible oxides such as TiO_2, CeO_2, and Nb_2O_5, after reduction at high temperature (about 773 K) (2). It was also demonstrated that this interaction could also affect the activity and selectivity of noble metals in different reactions, such as those involving molecules with carbonyl bonds (3, 4).

Recent results have shown that the SMSI effect can be due to both structural and electronic changes induced in the catalyst upon reduction at high temperature. In the case of ceria-supported noble metals, it has been shown that electronic metal–support interactions prevail for reduction temperatures up to 773 K, whereas metal decoration by partially reduced oxide has been observed by high-resolution transmission microscopy after reduction at 973 K (5).

[1] To whom correspondence should be addressed. Fax: +34 965 90 34 54. E-mail: asepul@ua.es.

The existence of strong metal–support interaction in ceria-supported or ceria-promoted noble metal catalysts can be assessed not only by following the inhibition of the H_2 or CO chemisorption ability of the catalyst when the reduction temperature is increased, but also with the help of probe reactions such as hydrogenation reactions, for which both the activity and the selectivity are generally strongly dependent on the reduction temperature at which the catalyst is submitted. One of them is the hydrogenation of α,β-unsaturated aldehydes (6, 7). These compounds contain two functionalities able to be hydrogenated: the hydrogenation of the olefinic C=C bond yields the saturated aldehyde, whereas the hydrogenation of the carbonyl C=O bond yields the unsaturated alcohol. The former reaction is more favored on platinum catalysts from both thermodynamic and kinetics points of view. However, it has been reported that platinum promotion by ceria enhances selectivity toward the hydrogenation of the carbonyl bond when the catalyst is reduced at high temperature (about 773 K) (7–10). Defect sites at the platinum–oxide interface, which are able to activate the C=O bond, as well as electronic effects on platinum have been postulated as responsible for this behavior. Furthermore, the role of the formation of Ce–Pt alloy phases after reduction at higher temperature has also been taken into consideration (10).

In spite of the great amount of research devoted to the study of the SMSI effect in monometallic catalysts, and even in bimetallic systems with two noble metals (Pt and Rh, for instance), very scarce attention has been devoted to the interaction of ceria and other reducible oxides with bimetallic systems containing one noncatalytically active metal. The addition of a second metal to noble metal catalysts can modify their catalytic behavior in a wide range of reactions. It is the case, for example, of bimetallic Pt–Sn or Pt–Re catalysts used in naphtha refining processes. Some of these systems also show enhanced activity and selectivity, compared with that of monometallic platinum, in the hydrogenation of α,β-unsaturated aldehydes: Pt–Sn (11–14), Pt–Fe (15), Pt–Zn (16, 17), and so forth. Thus, it is interesting to study the SMSI effect between ceria and these bimetallic systems using the above-mentioned hydrogenation as a probe reaction, as both the catalytic activity and

0021-9517/02 $35.00

selectivity may be modified. This paper reports preliminary results, which are an estimation of the interaction induced upon the reduction treatment, of the effect of reduction temperature on the catalytic behavior of ceria-promoted monometallic platinum and bimetallic platinum–zinc catalysts in the vapor-phase hydrogenation of crotonaldehyde (2-butenal). Results obtained in the vapor-phase hydrogenation of toluene, a structure-insensitive reaction, are also included for the sake of comparison.

EXPERIMENTAL PART

Cerium dioxide dispersed on silica was prepared by impregnation of a commercial SiO_2 support (Silicagel, 0.2–0.6 mm, $S_{BET} = 400\ m^2 \cdot g^{-1}$, from Acros) with an aqueous solution of $Ce(NO_3)_3 \cdot 6H_2O$ (purity 99.95%, from Ventron) of the appropriate concentration to obtain a CeO_2 loading of 20 wt%. The excess solvent was removed by flowing N_2 through the slurry at 333 K. Then, the sample was calcined at 673 K for 4 h. Platinum and zinc were introduced by coimpregnation with acetone solutions of $[Pt(NH_3)_4](NO_3)_2$ and $Zn(NO_3)_2 \cdot 6H_2O$ (from Aldrich). These precursors were chosen in order to avoid the presence of chlorine in the final catalysts, as it has been reported that it can affect the catalytic behavior of this kind of systems (8, 10, 16). Excess solvent was removed as described above and the samples were then dried overnight at 383 K and calcined at 673 K for 4 h. A monometallic Pt/CeO_2–SiO_2 catalyst was prepared in a similar way for the sake of comparison. Platinum content in both samples was 1.1 wt%, and zinc content in the bimetallic catalyst was 0.6 wt%, as determined by AAS. These values correspond to a Zn/Pt atomic ratio of 1.6.

X-ray diffraction patterns of samples, reduced in flowing hydrogen at 473 and 773 K and then air exposed, were obtained with a JSO Debye-Flex 2002 system, from Seifert, fitted with a Cu cathode and a Ni filter, and using a $2^\circ\ min^{-1}$ scanning rate.

Temperature-programmed reduction (TPR) measurements on calcined catalysts were carried out in a U-shaped quartz reactor, using a 5% H_2/He gas flow of $50\ cm^3 \cdot min^{-1}$ and about 150 mg of catalyst. Hydrogen consumption was monitored by online mass spectrometry and calibrated by carrying out the reduction of CuO and assuming that it is completely reduced to metallic copper.

X-ray photoelectron spectra (XPS) were acquired with a VG-Microtech Multilab 3000 spectrometer equipped with a hemispherical electron analyzer and a Mg $K\alpha$ ($h = 1253.6$ eV, 1 eV $= 1.6302 \times 10^{-19}$ J) 300-W X-ray source. The powder samples were pressed into small Inox cylinders and then mounted on a sample rod placed in a pretreatment chamber and reduced in flowing H_2 for 1 h at 473 and 773 K before being transferred to the analysis chamber. Before recording the spectra, the sample was maintained in the analysis chamber until a residual pressure of ca. $5 \times 10^{-7}\ N \cdot m^{-2}$ was reached. The spectra were collected at a pass energy of 50 eV. The intensities were estimated by calculating the integral of each peak, after subtraction of the S-shaped background, and by fitting the experimental curve to a combination of Lorentzian (30%) and Gaussian (70%) lines. All binding energies (B.E.) were referenced to the C 1s line at 284.6 eV, which provided binding energy values with an accuracy of ±0.2 eV.

Before the determination of their catalytic behavior, the catalysts were reduced *in situ* under flowing hydrogen ($50\ cm^3 \cdot min^{-1}$) at 473 or 773 K for 10 h, at a heating rate of $5\ K\ min^{-1}$. Toluene hydrogenation was studied at 333 K, with a reactant mixture containing purified hydrogen and toluene (Aldrich, HPLC grade) in a H_2/C_7H_8 ratio of 36. Crotonaldehyde hydrogenation was performed at 353 K. The reduced catalysts were contacted with a reaction mixture (total flow: $50\ cm^3 \cdot min^{-1}$; H_2/CROALD ratio of 26) formed by passing a hydrogen flow through a thermostabilized saturator (293 K) containing the unsaturated aldehyde. In both cases, the reaction products were analyzed by online gas chromatography, using a Carbowax 20M 58/90 25 to 30-m capillary column to separate the reactants and the reaction products.

RESULTS AND DISCUSSION

Catalyst Characterization

Figure 1 shows the X-ray diffraction patterns of catalysts Pt/CeO_2–SiO_2 and Pt–Zn/CeO_2–SiO_2 after reduction in flowing hydrogen at 473 and 773 K and then being air exposed. It can be seen that from the structural point of view, the reduction temperature affects both catalysts in a similar way. The profiles show the diffraction peaks corresponding to the fluorite phase of ceria, although these peaks are more poorly defined after the reduction at high temperature. In a previous paper dealing with the preparation of carbon-supported Pt–CeO_2 catalysts it was observed that the increase in the reduction temperature from 623 to 973 K originated an increase in the intensity of the ceria diffraction peaks, and it was attributed to the sintering of the partially reduced ceria phase (8). However, opposite results were found in a Pt/CeO_2–SiO_2 catalyst, for which the increase in the reduction temperature from 473 to 773 K caused a more poorly defined XRD spectra (7). These results may be related to the presence of silica as support. González-Elipe *et al.* (18) proposed the presence of a cerium silicate-like amorphous structure in silica-doped ceria. More recently, Rochinni *et al.* (19) have shown the formation of a cerium silicate phase upon reduction of a CeO_2–SiO_2 mixed oxide in hydrogen, at temperatures ranging from 600 to 1200 K. On the other hand, Bensalem *et al.* observed a small increase in the cerium binding energies (XPS measurements) in silica-supported ceria compared

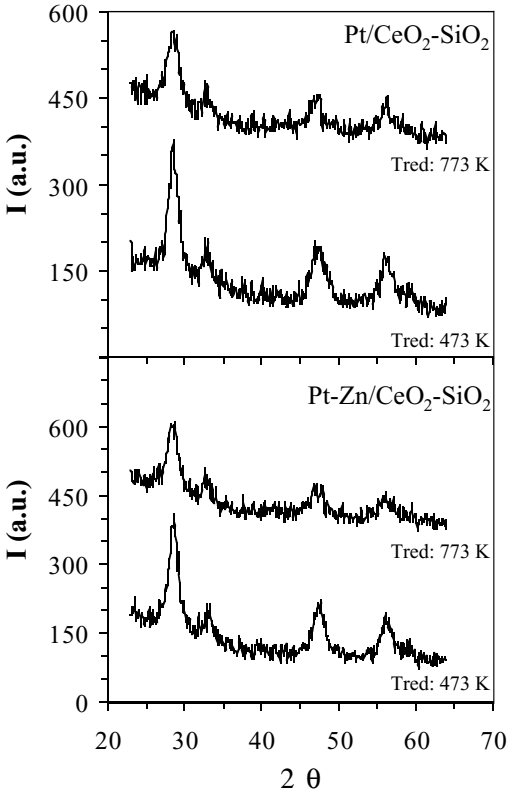

FIG. 1. X-ray diffraction patterns of catalysts $Pt/CeO_2–SiO_2$ and $Pt–Zn/CeO_2–SiO_2$ reduced at 473 and 773 K.

to bulk ceria (20). Although they noticed the possibility of being due to the formation of a new phase, they finally ascribed this observation to the coordinative unsaturation of surface cerium ions as a consequence of the very small particle size (from 1 to 8.5 nm).

In conclusion, although the more poorly defined XRD diffraction peaks of ceria in the catalysts after reduction at 773 K could be the result of the partial reaction of ceria with silica to form an amorphous silicate-like compound, it may also be originated by a small redispersion of the partially reduced ceria particles. In fact, the estimation of the mean particle sizes from the (111) line broadening of ceria gives values of 5.8 and 6.1 nm for the mono- and bimetallic catalysts, respectively, after reduction at 473 K, and of 4.3 and 5.1 nm after reduction at 773 K. No peaks corresponding to platinum can be observed in the XRD patterns, which is indicative of the presence of very small metal particles.

Figure 2 shows the temperature-programmed reduction profiles (H_2 consumption) obtained with the monometallic and the bimetallic catalysts. The TPR profile of $Pt/CeO_2–SiO_2$ shows three reduction peaks. The first one, centered at 365 K, is assigned to the surface reduction of CeO_2 in close contact with the metal, as well as to the breakdown of $Pt–O–CeO_2$ species formed upon calcination. The second peak, at about 640 K, corresponds to the surface reduction of CeO_2 that is not so close to platinum and, in this way, is less affected by hydrogen spillover from the metallic surface. Finally, the third broad peak, at about 1000 K, can be assigned to the reduction of bulk CeO_2. This profile is similar to those found in the literature (7, 21). However, the TPR profile of the bimetallic $Pt–Zn/CeO_2–SiO_2$ catalyst does not show the peak at the intermediate temperature. The intense low-temperature reduction peak is shifted to a slightly higher temperature compared with that of the monometallic catalyst (377 K) and it is accompanied by a shoulder at 447 K that may include the reduction of zinc oxide. These results are indicative of a higher interaction between the metallic phase and cerium dioxide in this catalyst, which modifies the redox behavior of the promoter.

The Pt 4f level X-ray photoelectron spectra for the fresh and reduced catalysts are compared in Figs. 3a (monometallic $Pt/CeO_2–SiO_2$) and 3b (bimetallic $Pt–Zn/CeO_2–SiO_2$). Two broad bands appear which correspond to the Pt $4f_{7/2}$ and Pt $4f_{5/2}$ levels. In a first approach, the broadness of the bands could be attributed to charge effects on the samples during the XPS measurement, as they were not compensated for by the use of a flood gun. If this is so, the XPS spectra indicate a shift of the Pt 4f binding energy toward lower values as the reduction temperature is increased. The shift is slightly more important for the bimetallic catalyst, and it is indicative of platinum reduction. However, the broad peaks may also be due to the overlapping of individual peaks corresponding to platinum species with slightly different electronic states. In fact, the broad experimental peaks are not strictly symmetrical, which could be explained by a different contribution of the individual peaks. In this

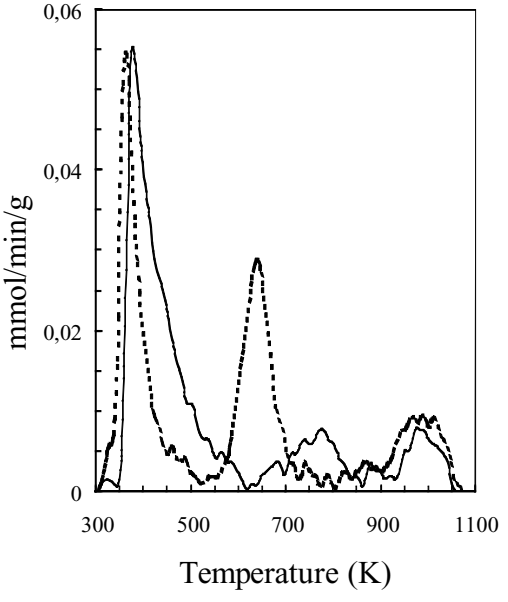

FIG. 2. TPR curves (H_2 consumption) for $Pt/CeO_2–SiO_2$ (dotted line) and $Pt–Zn/CeO_2–SiO_2$ (full line) catalysts.

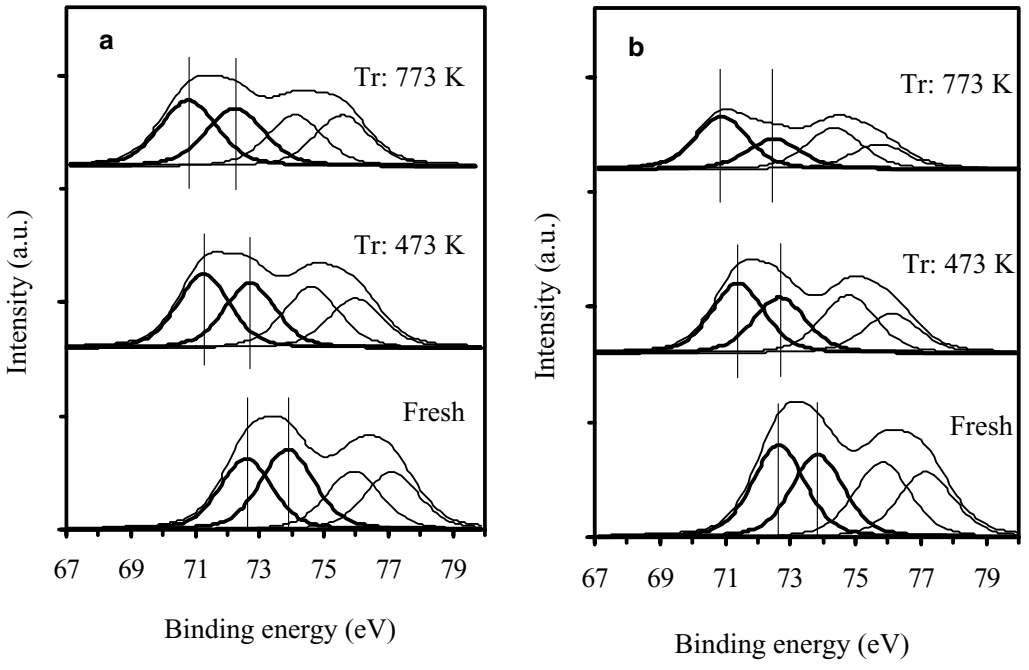

FIG. 3. XPS Pt 4f spectra of the fresh and reduced catalysts. (a) $Pt/CeO_2–SiO_2$; (b) $Pt–Zn/CeO_2–SiO_2$.

way, the main experimental Pt $4f_{7/2}$ peak has been deconvoluted into two components. Their binding energies and their relative contribution to the main peak, as well as the Pt/Si, Pt/Ce, and Pt/Zn XPS atomic ratios, are reported in Table 1. This table also reports the Si $2p_{3/2}$ binding energies obtained for the two catalysts after the different treatments. The same value has been obtained in all cases (104.2 eV), which is assigned to silicium in SiO_2.

Only small differences can be observed between the XP spectra of the mono- and the bimetallic catalysts, the main one being that, whatever the reduction treatment, the intensity of the peak placed at a lower binding energy is always higher for the bimetallic Pt–Zn catalyst. For the fresh samples the two peaks are centered at binding energies corresponding to Pt(II) species, and they are shifted toward lower binding energies as the reduction temperature increases. After reduction at 473 K, the peak at 72.7 eV still indicates the presence of Pt(II) species, and the one centered at 71.3 eV could correspond to Pt^0 species in an electron-deficient state. After reduction at 773 K both peaks are further shifted to lower binding energies; this indicates a higher reduction degree. On the other hand, the differences in intensity between both peaks increase with the reduction temperature, from 473 to 773 K, only for the bimetallic $Pt–Zn/CeO_2–SiO_2$ catalyst; this is indicative of a higher amount of platinum in a more reduced state in this sample.

TABLE 1

Catalyst Characterization by XPS

Catalyst	Reduct. Temp. (K)	Pt/Si	Pt/Zn	Pt/Ce	Ce/Si	B.E. Si $2p_{3/2}$ (eV)	B.E. Pt $4f_{7/2}$ (eV)	B.E. Ce u''' (eV)	Ce(III) (%)
$Pt/CeO_2–SiO_2$	—-	0.0042	—	0.15	0.0027	104.2	72.6 (46) 73.9 (54)	917.4	24
	473	0.0035	—	0.12	0.0029	104.2	71.3 (53) 72.7 (47)	917.4	33
	773	0.0034	—	0.10	0.0035	104.2	70.8 (53) 72.2 (47)	917.2	46
$Pt–Zn/CeO_2–SiO_2$	—-	0.0038	1.7	0.12	0.0031	104.2	72.6 (53) 73.8 (47)	917.2	28
	473	0.0037	2.2	0.12	0.0030	104.2	71.3 (56) 72.7 (44)	917.2	36
	773	0.0023	1.8	0.09	0.0027	104.2	70.9 (63) 72.5 (37)	917.1	49

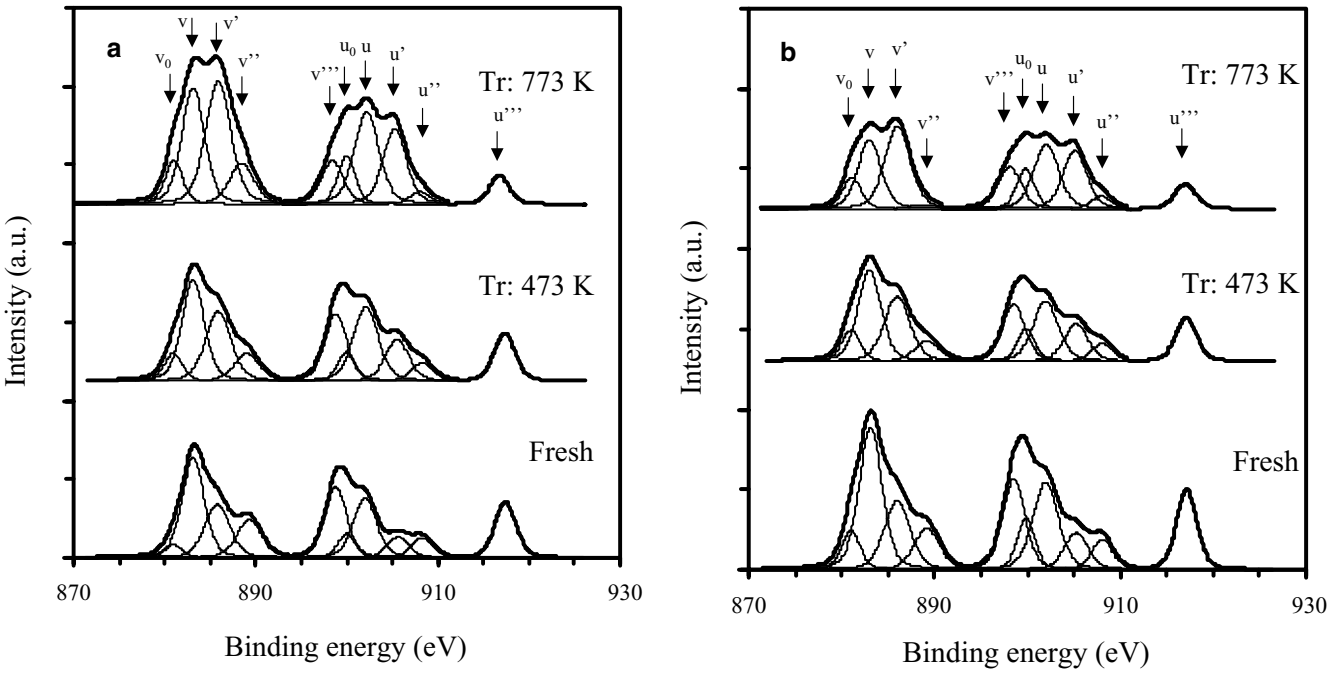

FIG. 4. XPS Ce 3d spectra of the fresh and reduced catalysts. (a) $Pt/CeO_2–SiO_2$; (b) $Pt–Zn/CeO_2–SiO_2$.

The possibility of Pt–Zn alloy formation in this kind of system has been addressed by several authors. Consonni *et al.* (16) observed that a PtZn alloy was formed in a Pt/ZnO catalyst, prepared with H_2PtCl_6 as the platinum precursor, after reduction at only 473 K; however, alloy formation was not observed when the Pt precursor was $[Pt(NH_3)_4](NO_3)_2$ unless the catalyst was reduced at 773 K. In a similar way, Zawadzki *et al.* (22) reported the formation of a Pt_3Zn alloy after reduction at 573 K of a $Pt/ZnAl_2O_4$ catalyst, prepared from H_2PtCl_6, and the formation of a PtZn alloy when the reduction was carried out at 773 K. In both cases, evidence of the alloy formation was obtained by XRD analysis.

The X-ray diffraction patterns of catalysts $Pt/CeO_2–SiO_2$ and $Pt–Zn/CeO_2–SiO_2$ (Fig. 1) do not allow discerning any diffraction peak that could be ascribed to Pt, Zn, or a Pt–Zn alloy, as the metal contents are small. Furthermore, the XPS analysis does not allow reliable verification of the formation of Pt–Zn alloy phases in these catalysts. Evidence could be the slightly higher binding energy of platinum in the bimetallic catalyst after reduction at 773 K (70.9 and 72.5 eV compared to 70.8 and 72.2 eV in the monometallic $Pt/CeO_2–SiO_2$) (23), but the differences are too small to be trustworthy. On the other hand, the binding energy of the Zn $2p_{3/2}$transition for the fresh bimetallic catalyst presents a single band centered at 1022.4 eV, which can be unambiguously assigned to Zn(II) species. The same binding energy is obtained after reduction at 473 K, and the reduction at 773 K causes a small shift just to 1022.0 eV. The difficulty of assessing the oxidation state of zinc by XPS measurements is well recognized in the literature, as the binding energy of metallic zinc and Zn(II) are very close. In this case, the lower B.E. of zinc in the catalyst reduced at 773 K could be tentatively attributed to the presence of metallic zinc in this catalyst, but it is necessary to take into account the possibility that other factors may also apply for the small shift observed. It has also to be remarked that the analysis of the Zn LMM Auger transition, which is more sensitive to the oxidation state of zinc (24), does not supply any further information.

Figures 4a and 4b show the Ce 3d XP spectra obtained with catalysts $Pt/CeO_2–SiO_2$ and $Pt–Zn/CeO_2–SiO_2$, respectively, both in the fresh state and after *in situ* reduction at 473 and 773 K. The complexity of the spectra, which were first resolved by Burroughs *et al.* (25), arises from the hybridization between the Ce 4f levels and the O 2p states. The two sets of spin-orbital multiplets, corresponding to the $3d_{3/2}$ and $3d_{5/2}$ contributions, are labeled u and v, respectively, and up to four peaks for each contribution can be obtained by a curve-fitting analysis (26), as shown in Figs. 4a and 4b. The peaks labeled v and v'' have been assigned to a mixing of Ce $3d^9\ 4f^2\ O\ 2p^4$ and Ce $3d^9\ 4f^1\ O\ 2p^5$ Ce(IV) final states, and the peak denoted v''' corresponds to the Ce $3d^9\ 4f^0\ O\ 2p^6$ Ce(IV) final state. On the other hand, lines v_0 and v' are assigned to the Ce $3d^9\ 4f^2\ O\ 2p^5$ and the Ce $3d^9\ 4f^1\ O\ 2p^6$ of Ce(III). The same assignation can be applied to the u structures, which correspond to the Ce $3d_{3/2}$ levels. Two different approaches have been followed to evaluate the degree of ceria reduction from the XP spectra. On one hand, some authors have used the

percentage of area of the u''' peak in the total Ce 3d region to describe the total amount of Ce(IV) in the sample (27–29). However, it has been shown that this procedure leads to erroneous quantitative results (30). The second approach takes into consideration the relative intensity of the u_0 (v_0) and u' (v') peaks, as representative of Ce(III), in the total Ce 3d region (26, 31, 32). In this way, the degree of ceria reduction can be calculated, after deconvolution of the experimental spectra, from the ratio between the sum of the intensities of the u_0, u', v_0, and v' bands and the sum of the intensities of all the bands (26):

$$\text{Ce(III)}(\%) = \frac{100 \cdot [\text{S}(u_0) + \text{S}(u') + \text{S}(v_0) + \text{S}(v')]}{\sum[\text{S}(u) + \text{S}(v)]}.$$

The percentages of reduction of Ce for the two catalysts after the different reduction treatments are reported in Table 1. It can be seen that there is a certain amount of Ce(III) even in the fresh catalysts. It has been shown that Ce(IV) ions can be partially reduced during XPS experiments (31, 33). One of the parameters that mainly affect the photoreduction of CeO_2 during XPS analysis is its crystallinity, which is affected in such a way that amorphous cerium oxide samples are reduced more extensively than crystalline materials (34). Taking into account the fact that the same support has been used for the preparation of the Pt monometallic and Pt–Zn bimetallic catalysts, and that the XPS analysis has been carried under the same conditions, it can be assumed that Ce(IV) photoreduction by effect of the X-ray beam should be similar for both catalysts, and in this way, differences in reducibility are only due to their distinctive chemical composition. Data in Table 1 show that the extent of Ce(IV) reduction increases with the reduction temperature, and that the reducibility of ceria in the bimetallic Pt–Zn catalysts is slightly higher than that of the monometallic Pt sample. On the other hand, the binding energies of the Ce u''' peak are also reported in Table 1. Accordingly to literature data (31) the values are around 917.2 eV, with no significant shifts due to the reduction temperature or the presence of zinc.

The XPS atomic Ce/Si ratios of the two catalysts after the different reduction treatments are also reported in Table 1. For the monometallic sample, this ratio increases from 0.0029 to 0.0035 when the reduction temperature is increased from 473 to 773 K. This implies a higher amount of surface cerium ions that can be related to a decrease in the mean particle size of the supported oxide. This explanation is corroborated by XRD results, which show a decrease in the size of ceria particles from 5.8 to 4.3 nm. However, the increase in surface cerium ions with the increase in reduction temperature is not observed in the bimetallic catalysts, in spite of the fact that a reduction in particle size is also deduced from XRD results. In this case, the lower Ce/Si atomic ratio obtained by XPS can be attributed to the coverage of ceria (or partially reduced ceria) particles by metallic zinc. A similar effect is observed for platinum. In the monometallic catalyst, the XPS Pt/Si atomic ratio remains nearly unchanged when the reduction temperature is increased, thus indicating that platinum does not sinter to a significant extent after reduction at high temperature. However, the XPS Pt/Si atomic ratio does strongly decrease in the bimetallic catalyst when the reduction temperature is increased (from 0.0037 to 0.0023). As a different sintering behavior of platinum in this bimetallic catalyst seems unlikely, this decrease is attributed to a dilution effect of zinc on surface platinum atoms, with the possibility of the formation of alloy phases. The coverage or decoration of platinum particles by patches of partially reduced ceria after high-temperature reduction could also account for the decrease in surface platinum, as detected by XPS. HRTEM studies have show that this decoration effect does not take place in monometallic Pt catalysts unless much higher reduction temperatures (around 973 K) are used (5), but this may not be so in the presence of other metals, such as Zn.

Catalytic Behavior

The assessment of metallic dispersion in supported metallic catalysts containing ceria by gas adsorption measurements is not easy, given that the promoter is also able to chemisorb hydrogen and CO at room temperature. An estimation of the amount of platinum surface atoms in these systems can be achieved by determining their catalytic activity in a structure-insensitive reaction. In this way, benzene hydrogenation (35) and cyclohexane dehydrogenation (36) have already been used as test reactions to estimate the amount of metal atoms exposed in ceria-promoted noble metal catalysts. Whereas in the latest case the highest reduction temperature used was 573 K, a good correlation was obtained in the first case between the amount of exposed metal atoms determined by benzene hydrogenation and that obtained from hydrogen chemisorption in chlorine-containing samples reduced at 773 K, which is high enough as to induce the SMSI effect. However, it is necessary to bear in mind that the structure-insensitive character of these reactions may be affected if any electronic effect of partially reduced ceria on the metal particles is generated upon reduction at high temperature. This effect can affect in a similar way the activity for benzene hydrogenation and the ability for hydrogen chemisorption.

The effect of the reduction temperature on the catalytic activity of Pt/CeO_2–SiO_2 and Pt–Zn/CeO_2–SiO_2 for an structure-insensitive reaction, toluene hydrogenation, was tested at 333 K, after treating the catalysts in flowing hydrogen at 473 or 773 K. The monometallic Pt/CeO_2–SiO_2 shows the highest activity after reduction at both low (473 K, 139 μmol of methyl cyclohexane $\cdot\, s^{-1} \cdot g\,Pt^{-1}$) and high temperature (773 K, 82 μmol of methyl cyclohexane $\cdot\, s^{-1} \cdot g\,Pt^{-1}$). Studies on benzene hydrogenation over

ceria-supported metals such as Rh (37), Pd (38), Ir (39), and Pt (7, 40) have shown that reduction temperature strongly affects catalytic activity, in such a way that a very strong decrease is observed after reduction at 773 K. These results have been explained on the basis of different phenomena, as the formation of metal–cerium alloys and the sintering of the metal particles. Platinum–cerium alloys have only been detected after reduction at temperatures much higher than those used in this study, around 973 K (10, 41). With regard to the possibility of platinum sintering, XPS data reported in Table 1 show that the atomic Pt/Si ratios detected by this technique in the monometallic catalyst, which can be regarded as an estimation of platinum dispersion, are very close irrespective of the reduction temperature. Thus, the sintering of platinum as a consequence of the reduction treatment at 773 K can be discarded as the origin of its lower activity for toluene hydrogenation.

On the other hand, the bimetallic Pt–Zn/CeO_2–SiO_2 catalyst shows very low catalytic activity. After reduction at 473 K, when a strong interaction with ceria is not expected, the catalytic activity is only 6 $\mu mol \cdot s^{-1} \cdot gPt^{-1}$. This value is 23 times lower than that of the monometallic catalyst and can be explained by a dilution effect of zinc in this catalyst, likely by alloy formation, or by surface segregation of zinc, which decreases the number of surface platinum atoms. As for the monometallic sample, reduction of the bimetallic catalyst at high temperature produces a decrease in catalytic activity (0.8 $\mu mol \cdot s^{-1} \cdot gPt^{-1}$) for this reaction, although it is much stronger in this case.

The effect of the presence of zinc and the reduction temperature on the catalytic behavior of these samples in the vapor-phase hydrogenation of crotonaldehyde is very different from that observed in toluene hydrogenation, mainly for the bimetallic Pt–Zn catalyst. Figure 5a shows the evolution of the overall activity (micromoles of crotonaldehyde transformed per gram of platinum per second) of catalyst Pt/CeO_2–SiO_2 in that reaction as a function of time on stream at 353 K, after being reduced at 473 and 773 K. These values were obtained when the carbon balance was achieved, i.e., once the amount of crotonaldehyde leaving the reactor matched that fed minus that transformed into the products. It can be seen that after an initial deactivation during the first 25 min, the activity remains rather stable with time on stream. On the other hand, reduction at high temperature causes a decrease in catalytic activity, close to that observed for toluene hydrogenation although to a somewhat lesser extent. In fact, the ratio between the initial activity for crotonaldehyde hydrogenation and that for toluene hydrogenation is 1.4 for the catalyst reduced at 473 K and 1.59 after reduction at 773 K. These results are similar to those obtained in a previous study on the vapor-phase hydrogenation of crotonaldehyde over a Pt/CeO_2–SiO_2 with 5 wt% CeO_2 and prepared with a chlorinated platinum precursor (H_2PtCl_6) (7). It is also worth mentioning that the effect of the reduction temperature was the opposite for a Pt/CeO_2 catalyst, i.e., the catalytic activity strongly increased with the increase in the reduction temperature from 473 to 773 K (7). Abid *et al.* also observed a decrease in the catalytic activity for the title reaction on 5% Pt/CeO_2 catalysts, prepared with chlorinated and chlorine-free precursors, when the reduction temperature was increased from 473 to 973 K (10). However, the comparison with our catalysts is not straightforward due to the difference between the highest reduction temperatures used (973 vs 773 K).

Figure 5b plots the evolution of the overall activity (micromoles of crotonaldehyde transformed per gram of platinum per second) of catalyst Pt–Zn/CeO_2–SiO_2 in crotonaldehyde hydrogenation as a function of time on stream at 353 K, after being reduced at 473 and 773 K. The

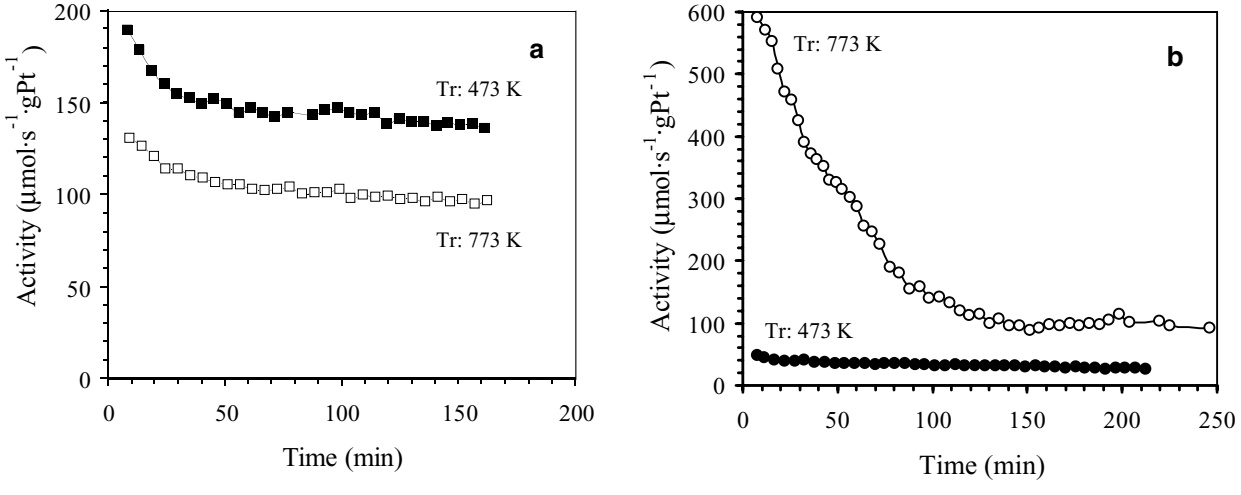

FIG. 5. Evolution of catalytic activity for crotonaldehyde hydrogenation for catalysts as a function of time on stream at 353 K, after reduction at 473 or 773 K. (a) Pt/CeO_2–SiO_2; (b) Pt–Zn/CeO_2–SiO_2.

distinctive behavior of this system compared to that of the monometallic catalyst is clearly evidenced. After reduction at low temperature (473 K) its catalytic activity is lower than that obtained for $Pt/CeO_2–SiO_2$, although the decrease in activity for this reaction is much lower than that observed in toluene hydrogenation. If, as discussed above, the lower activity of the bimetallic catalyst for toluene hydrogenation is due to a diluting effect of zinc on the surface platinum atoms, this effect seems to be not so detrimental for crotonaldehyde hydrogenation. In fact, it has been reported that Pt/ZnO catalysts show high performance in this reaction (16), and it has been explained on the basis of the formation of PtZn alloy phases, in which $Pt^{\delta-}–Zn^{\delta+}$ entities are formed which favor the adsorption of crotonaldehyde by the carbonyl group and, in this way, promote its hydrogenation to produce crotyl alcohol. A similar effect has been found in Pt–Zn catalysts supported on zeolite NaX (17).

Reduction of the bimetallic catalyst at 773 K produces a drastic increase in activity for crotonaldehyde hydrogenation, as can be seen in Fig. 5b, with the initial activity going from 100 $\mu mol \cdot s^{-1} \cdot gPt^{-1}$ after reduction at 473 K to near 600 $\mu mol \cdot s^{-1} \cdot gPt^{-1}$. The catalyst suffers an important deactivation during the first 100 min on stream, then reaches a steady state value which is about five times higher than that obtained after reduction at 473 K. This effect is completely opposite that observed in toluene hydrogenation, where a strong deactivation was obtained after reduction at high temperature. In this way, the presence of zinc in this bimetallic catalyst has a very important role in determining its catalytic behavior in a reaction such as the hydrogenation of crotonaldehyde. Not only does this role apply to catalytic activity it also, as it is discussed below, affects catalytic selectivity.

The products obtained under the conditions used in this study are butyraldehyde (formed by the hydrogenation of the C=C bond), crotyl alcohol (but-2-en-ol, formed by the hydrogenation of the carbonyl C=O bond), butanol (formed upon hydrogenation of the primary products butyraldehyde and crotyl alcohol), and the light hydrocarbons butane (formed through butanol hydrogenation) and propane, which is the result of crotonaldehyde and butyraldehyde decarbonylation reactions. In the case of the monometallic $Pt/CeO_2–SiO_2$ catalyst, butanol is not detected, and the amount of light hydrocarbons is similar during both runs, irrespective of the reduction temperature, and is lower than 5% molar fraction; consequently, a high selectivity to crotyl alcohol means a low selectivity for the hydrogenation of the olefinic C=C bond yielding butyraldehyde. The selectivity to crotyl alcohol (CROALC) (molar fraction, %) is plotted in Fig. 6 as a function of the conversion degree in reaction at 353 K after reduction at both low (473 K) and high (773 K) temperature. Higher conversion levels are obtained at the first stages of the reaction; thereafter, deactivation decreases the conversion degree. It

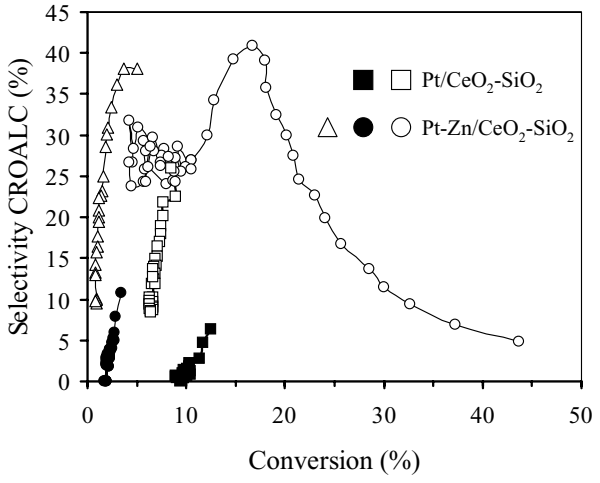

FIG. 6. Evolution of selectivity to crotyl alcohol as a function of the conversion degree. (Solid symbols) Catalysts reduced at 423 K; reaction at 353 K. (Open symbols) Catalysts reduced a 773 K; reaction at 353 K except Δ, for which reaction was at 313 K.

can be seen that reduction at high temperature produces a strong increase in selectivity to crotyl alcohol. This effect has been previously reported and it has been related to the onset of the strong metal–support interaction (SMSI) effect in this kind of catalysts (7, 8) and, for higher reduction temperatures, to the formation of $CePt_5$ alloy particles (10). Reduction at 773 K forms oxygen vacancies, or coordinatively unsaturated Ce^{3+} cations, on the ceria promoter close to the platinum particles; then, the interaction of the oxygen atom of the carbonyl group in crotonaldehyde with these vacancies can activate it, which favors its hydrogenation by hydrogen atoms adsorbed on the platinum particles or spilt over from them to the platinum–ceria interface. On the other hand, the partial reduction of ceria may also electronically affect the platinum particles, which modifies their catalytic behavior and hinders their ability for hydrogenation of the olefinic C=C bond, which in turns favors the production of crotyl alcohol.

The selectivity of the bimetallic $Pt–Zn/CeO_2–SiO_2$ catalysts to the production of crotyl alcohol is also plotted in Fig. 6 as a function of the conversion degree. After reduction at 473 K the initial selectivity is only slightly higher than that of the monometallic catalyst, although measured at an inferior conversion degree due to its lower activity. It must be remarked that the yield of butanol is also higher with this catalyst, remaining steady at around a 10% molar fraction during the reaction run. The behavior is completely different after reduction at 773 K. In this case, as is shown in Fig. 6, the initial selectivity to crotyl alcohol is only about 5%, but it increases with time on reaction up to a 40% molar fraction at 16% conversion (60 min on stream). Then, it decreases further and finally stabilizes at about 27%. However, the low initial selectivity to crotyl

alcohol is not matched here with a higher production of butyraldehyde (selectivity: 62% molar fraction) but is accompanied by relatively high selectivity to butanol (33% molar fraction), which decreases with time on stream as selectivity to crotyl alcohol increases. These results indicate that a secondary reaction is taking place on this catalyst during the first 60 min on stream, namely the hydrogenation of the initial products, butyraldehyde and mainly crotyl alcohol, to yield butanol. As the catalyst deactivates and the conversion degree decreases, this secondary reaction is less favored and selectivity to crotyl alcohol increases. But, on the other hand, the deactivation involves sites where the carbonyl bond is preferentially hydrogenated, and the loss of these sites makes the selectivity to crotyl alcohol decrease further, until it reaches approximately 27%, remaining there until the end of the reaction run. In order to check this proposed explanation, the reaction was also carried out at 313 K with the bimetallic catalyst reduced at 773 K, and the selectivity data obtained are also shown in Fig. 6. The initial conversion degree is much lower in this case, and butanol was not detected even at the first stages of the reaction. It is in these first stages when the maximum selectivity to crotyl alcohol is obtained (38%), as it is not further hydrogenated to butanol; however, it quickly drops as the catalyst deactivates.

The promotional effect of electropositive metals (Sn, Ge, Zn) on platinum for the selective hydrogenation of α,β-unsaturated aldehydes has been explained both by the formation of alloy phases and by the effect of oxidized species of the promoter metal on the oxygen atom of the carbonyl bond. Both explanations are not conflicting, as oxidized species have been reported to be formed in Pt–Sn catalysts upon reaction conditions, which favors the preferential hydrogenation of the carbonyl bond (13, 42). In a recent study dealing with Pt/ZnO catalysts prepared with different platinum precursors, Consonni *et al.* (16) showed that a temperature higher than 473 K was necessary to partially reduce the ZnO support when $[Pt(NH_3)_4](NO_3)_2$ was used as Pt precursor, and in this way, the formation of Pt–Zn alloys was likely only at these higher temperatures. Consequently, these authors observed that the selectivity to crotyl alcohol increased by reducing their catalyst at higher temperatures, achieving 49% selectivity after reduction at 673 K whereas it was only 21% after reduction at 473K.

Following these results, it could be then assumed that Pt–Zn alloy was formed in the bimetallic Pt–Zn/CeO_2–SiO_2 catalyst after reduction at 773 K. However, this assumption is not enough to explain the distinctive behavior of this catalyst. In their study of Pt/ZnO catalysts, Consonni *et al*. observed a decrease in activity at 353 K from 7 to 1.5 $\mu mol \cdot s^{-1} \cdot g^{-1}$ of Pt when the reduction temperature was increased from 473 to 673 K, i.e., when the formation of Pt–Zn alloy was favored. In contrast, the catalytic activity of Pt–Zn/CeO_2–SiO_2 strongly increased with the reduction temperature. Thus, the role of partially reduced ceria has also to be taken into account.

The role of ceria and other reducible oxides (TiO_2, etc.,) as promoter in this kind of reaction has been attributed to the interaction of the oxygen atom in the carbonyl bond of the unsaturated aldehyde with oxygen vacancies or Ce^{3+} cations created upon reduction at high temperature (7–10, 43). Under this assumption, the much higher activity and selectivity of the bimetallic Pt–Zn catalyst compared to the monometallic one could be explained on the basis of a higher reducibility of the ceria promoter in the bimetallic catalyst. This yields a higher amount of oxygen vacancies after reduction at 773 K, which would be able to weaken the carbonyl bond by interacting with its oxygen atom. In fact, XPS results have shown that a slightly higher amount of CeO_2 is effectively reduced in the bimetallic catalyst (Table 1). However, it seems that the relative amounts of Ce(III) in both catalysts are too close to explain, by itself, the extremely different catalytic behavior.

The onset of strong metal–support interaction (SMSI) effect in ceria-supported noble metals after reduction at high temperature is characterized by several features, such as suppression of chemisorption ability and modification of its catalytic behavior. The origin of this effect is still a matter of debate: (i) formation of Pt–Ce alloy, (ii) decoration of platinum particles by patches of partially reduced ceria, or (iii) electronic effects on platinum due to the partial reduction of ceria. The formation of Pt–Ce alloy and the metal decoration effect have only been evidenced after reduction of Pt/CeO_2 catalysts at temperatures higher than 773 K (around 973 K) (5, 10, 44). In this way, the electronic-effect argument stays as the main origin of the SMSI effect in ceria-supported platinum catalysts. Electron density would be transferred from the metal particles to the partially reduced ceria to stabilize the oxygen vacancies created upon reduction. The electron deficiency in platinum will then cause a decrease in its ability to chemisorp hydrogen and also a decrease in catalytic activity in reactions such as benzene and toluene hydrogenation. The situation is more complex in bimetallic systems such as the Pt–Zn catalyst. In this case, platinum is affected by both the ceria-promoter and the zinc species, which may be in an oxidized state or in metallic state. If a Pt–Zn alloy is formed upon reduction at high temperature, the interaction of partially reduced ceria with the alloy particles may modify their catalytic behavior to a different extent than with monometallic platinum particles. On the other hand, if zinc remains in an oxidized state after reduction at 773 K, there would be a higher number of catalytic Lewis acid sites ($Zn^{\delta+}$ and oxygen vacancies in partially reduced ceria) close to platinum particles which are able to interact with the oxygen atom of the carbonyl bond. This would favor its preferential hydrogenation to yield the unsaturated alcohol. Further

studies are being carried out with this and similar bimetallic systems to try to clarify the origin of the interesting catalytic behavior reported here.

CONCLUSIONS

The study reported in this paper shows that the effect of reduction temperature on the catalytic behavior of ceria-promoted platinum catalysts is much stronger in the presence of Zn. The catalytic activity for toluene hydrogenation is greatly decreased after reduction at high temperature (773 K) compared with the results obtained after reduction at low temperature (473 K). In the case of the vapor-phase hydrogenation of crotonaldehyde, the overall catalytic activity increases significantly after reduction at 773 K in the zinc-containing catalyst, and furthermore, the selectivity toward the hydrogenation of the carbonyl bond is improved.

ACKNOWLEDGMENTS

The authors are grateful to the M.E.C (Spain) for a Ph.D. studentship (J.S.A.) and to C.I.C.Y.T for financial support (Project BQU 2000-0467).

REFERENCES

1. Tauster, S. J., Fung, S. C., and Garten, R. L., *J. Am. Chem. Soc.* **100**, 170 (1978).
2. Tauster, S. J., and Fung, S. C., *J. Catal.* **56**, 29 (1978).
3. Vannice, M. A., *in* "Catalysis-Science and Technology" (J. R. Anderson and M. Boudart, Eds.), Vol. 3, Chap. 3, pp. 140–194. Springer-Verlag, Berlin, 1982.
4. Vannice, M. A., Twu, C. C., and Moon, S. H., *J. Catal.* **79**, 70 (1983).
5. Bernal, S., Calvino, J. J., Cauqui, M. A., Gatica, J. M., Larese,C., Pérez-Omil, J. A., and Pintado, J. M., *Catal. Today* **50**, 175 (1999).
6. Vannice, M. A., and Sen, B., *J. Catal.* **115**, 65 (1989).
7. Sepúlveda-Escribano, A., Coloma, F., and Rodríguez-Reinoso, F., *J. Catal.* **178**, 649 (1998).
8. Sepúlveda-Escribano, A., Silvestre-Albero, J., Coloma, F., and Rodríguez-Reinoso, F., *Stud. Surf. Sci. Catal.* **130**, 1013 (2000).
9. Abid, M., and Touroude, R., *Catal. Lett.* **69**, 139 (2000).
10. Abid, M., Ehret, G., and Touroude, R., *Appl. Catal.* **217**, 219 (2001).
11. Marinelli, T. B. L. W., Nabuurs, S., and Ponec, V., *J. Catal.* **151**, 431 (1995).
12. Coloma, F., Sepúlveda-Escribano, A., Fierro, J. L. G., and Rodríguez-Reinoso, F., *Appl. Catal. A* **136**, 231 (1996).
13. Margitfalvi, J. L., Vankó, Gy., Borbáth, I., Tompos, A., and Vertés, A., *J. Catal.* **190**, 474 (2000).
14. Homs, N., Llorca, J., Ramírez de la Piscina, P., Rodríguez-Reinoso, F., Sepúlveda-Escribano, A., and Silvestre-Albero, J., *Phys. Chem. Chem. Phys.* **3**, 1782 (2001).
15. Beccat, P., Bertolini, J. C., Gauthier, Y., Massardier, J., and Ruiz, P., *J. Catal.* **126**, 451 (1990).
16. Consonni, M., Jokic, D., Yu Murzin, D., and Touroude, R., *J. Catal.* **188**, 165 (1999).
17. Sepúlveda-Escribano, A., Silvestre-Albero, J., Coloma, F., and Rodríguez-Reinoso, F., *Stud. Surf. Sci. Catal.* **135**, 29-P-15 (2001).
18. González-Elipe, A. R., Fernández, A., Holgado, J. P., Caballero, A., and Munuera, G., *J. Vac. Sci. Technol. A* **11**, 58 (1993).
19. Rochinni, E., Trovarelli, A., Llorca, J., Graham, G. W., Weber, W. H., Maciejewski, M., and Baiker, A., *J. Catal.* **194**, 461 (2000).
20. Bensalem, A., Bozon-Verduraz, F., Delamar, M., and Bugli, G., *Appl. Catal. A* **121**, 81 (1995).
21. Trovarelli, A., *Catal. Rev.–Sci. Eng.* **38**, 439 (1996).
22. Zawadzki, M., Mista, W., and Lepinski, L., *Vacuum* **63**, 291 (2001).
23. Larese, C., Campos-Martin, J. M., and Fierro, J. L. G., *Langmuir* **16**, 10294 (2000).
24. Green, B. E., Sass, C. S., Germinario, L. T., Wehner, P. S., and Gustafson, B. L., *J. Catal.* **140**, 406 (1993).
25. Burroughs, P., Hammett, A., Orchard, A. F., and Thornton, G., *J. Chem. Soc. Dalton Trans.* 1686 (1976).
26. Laachir, A., Perrichon, V., Badri, A., Lamotte, J., Catherine, E., Lavalley, J. C., El Fallal, J., Hilaire, L., le Normand, F., Quéméré, E., Sauvion, G. N., and Touret, O., *J. Chem. Soc. Faraday Trans.* **87**, 1601 (1991).
27. Shyu, J. Z., Otto, K., Watkins, W. L. H., Graham, G. W., Belitz, R. K., and Gandhi, H. S., *J. Catal.* **114**, 23 (1988).
28. Shyu, J. Z., Weber, W. H., and Gandhi, H. S., *J. Phys. Chem.* **92**, 4964 (1988).
29. Noronha, F. B., Fendley, E. C., Soares, R. R., Alvarez, W. E., and Resasco, D. E., *Chem. Eng. J.* **82**, 21 (2001).
30. Kotani, A., Jo, T., and Parlebas, J. C., *Adv. Phys.* **37**, 37 (1989).
31. Francisco, M. S. P., Mastelaro, V. R., Nascente, P. A. P., and Florentino, A. O. A., *J. Phys. Chem. B* **105**, 10515 (2001).
32. Ernst, B., Hilaire, L., and Kiennemann, A., *Catal. Today* **50**, 413 (1999).
33. Larsson, P.-O., and Andersson, A., *J. Catal.* **179**, 72 (1998).
34. Park, P. W., and Ledford, J. S., *Langmuir* **7**, 1794 (1996).
35. Fajardie, F., Tempére, J.-F., Djèga-Mariadassou, G., and Blanchard, G., *J. Catal.* **163**, 77 (1996).
36. Rogemond, E., Essayem, N., Frety, R., Perrichon, V., Primet, M., and Mathis, F., *J. Catal.* **166**, 229 (1997).
37. Bernal, S., Botana, F. J., Calvino, J. J., Cauqui, M. A., Cifredo, G. A., Jobacho, A., Pintado, J. M., and Rodríguez-Izquierdo, J. M., *J. Phys. Chem.* **97**, 4118 (1993).
38. Lepinski, L., Wolcyrz, M., and Okal, J., *J. Chem. Soc. Faraday Trans.* **91**, 507 (1995).
39. Da Silva, P. N., Guenin, M., Leclercq, C., and Frety, R., *Appl. Catal.* **54**, 203 (1989).
40. Meriadeau, P., Dutel, J. F., Dufaux, M., and Naccache, C., *Stud. Surf. Sci. Catal.* **11**, 95 (1991).
41. Bernal, S., Calvino, J. J., Gatica, J. M., Larese, C., López-Cartés, C., and Pérez-Omil, J. A., *J. Catal.* **169**, 510 (1997).
42. Coloma, F., Llorca, J., Homs, N., Ramírez de la Piscina, P., Rodríguez-Reinoso, F., and Sepúlveda-Escribano, A., *Phys. Chem. Chem. Phys.* **2**, 3063 (2000).
43. Bachiller-Baeza, B., Rodríguez-Ramos, I., and Guerrero-Ruiz, A., *Appl. Catal. A* **205**, 227 (2001).
44. Datye, A. K., Kalakkad, D. S., Yai, M. H., and Smith, D. J., *J. Catal.* **155**, 148 (1995).